

Received 26 March 2024; revised 2 July 2024; accepted 9 July 2024. Date of publication 17 July 2024; date of current version 20 August 2024. The review of this article was arranged by Editor Paolo Bonato.

Digital Object Identifier 10.1109/OJEMB.2024.3429294

Complex Hemodynamic Responses to Trans-Vascular Electrical Stimulation of the Renal Nerve in Anesthetized Pigs

FILIPPO AGNESI¹, LUCIA CARLUCCI¹, GIA BURJANADZE¹, FABIO BERNINI¹, KHATIA GABISONIA¹, JOHN W OSBORN², SILVESTRO MICERA^{3,4} (Fellow, IEEE), AND FABIO A. RECCHIA^{5,6,7}

¹Interdisciplinary Research Center "Health Science", Scuola Superiore Sant'Anna, Pisa 56127, Italy

²Department of Integrative Biology and Physiology, Medical School, University of Minnesota, Minneapolis, MN 55455 USA

³The BioRobotics Institute, Department of Excellence in Robotics & AI, Scuola Superiore Sant'Anna, Pisa 56127, Italy

⁴Bertarelli Foundation Chair in Translational NeuroEngineering, Centre for Neuroprosthetics and Institute of Bioengineering, École Polytechnique Fédérale de Lausanne (EPFL), Lausanne 1015, Switzerland

⁵Scuola Superiore Sant'Anna, Pisa 56127, Italy

⁶Lewis Katz School of Medicine, Cardiovascular Research Center, Temple University, Philadelphia, PA 19140 USA

⁷Institute of Clinical Physiology, National Research Council, Rome 00185, Italy

(*Silvestro Micera and Fabio A. Recchia contributed equally to this work.*)

CORRESPONDING AUTHOR: Fabio A. Recchia (e-mail: recchia@santannapisa.it).

This work was supported in part by Intramural Funding (FR), in part by FET Grant NEUHEART under Grant 824071 (SM), in part by NEXTGENERATIONEU (NGEU) and funded by the Ministry of University and Research (MUR), in part by the National Recovery and Resilience Plan (NRRP), through Project Tuscany Health Ecosystem (THE) (DN. 1553 11.10.2022) (SM) under Grant IEC500000017, in part by NEXTGENERATIONEU (NGEU) and funded by the Ministry of University and Research (MUR), and in part by the National Recovery and Resilience Plan (NRRP) through Project A Multiscale integrated approach to the study of the nervous system in health and disease (MNESYS) (DN. 1553 11.10.2022) (SM) under Grant PE0000006.

ABSTRACT The objective of this study was to characterize hemodynamic changes during trans-vascular stimulation of the renal nerve and their dependence on stimulation parameters. We employed a stimulation catheter inserted in the right renal artery under fluoroscopic guidance, in pigs. Systolic, diastolic and pulse blood pressure and heart rate were recorded during stimulations delivered at different intravascular sites along the renal artery or while varying stimulation parameters (amplitude, frequency, and pulse width). Blood pressure changes during stimulation displayed a pattern more complex than previously described in literature, with a series of negative and positive peaks over the first two minutes, followed by a steady state elevation during the remainder of the stimulation. Pulse pressure and heart rate only showed transient responses, then they returned to baseline values despite constant stimulation. The amplitude of the evoked hemodynamic response was roughly linearly correlated with stimulation amplitude, frequency, and pulse width.

INDEX TERMS Electrical stimulation, renal nerve, trans-vascular stimulation.

IMPACT STATEMENT Hemodynamic responses to renal nerve trans-vascular electrical stimulation appears more complex than previously reported, fine combinations of stimulation parameters will be useful in clinical neuromodulation of the renal artery.

I. INTRODUCTION

The kidneys are known to play a key role in the long-term arterial blood pressure (BP) regulation through two main mechanisms: production and release of renin and blood volume control by urinary sodium excretion. Renal innervation is of particular interest for its capacity to control renal function and to influence the activation state of the sympathetic system. In 1859 Claude Bernard

observed that severing the greater splanchnic nerve produced ipsilateral diuresis and that electrical stimulation of the peripheral stub produced ipsilateral antidiuresis [1]. Nowadays, it is well known that sympathetic efferent fibres convey signals from the hypothalamic centers to the kidneys, while afferent fibres originating from the kidneys transmit sympatho-excitatory signals towards autonomic regulatory nuclei in the central nervous system. The interplay

between sympathetic nervous system and kidneys is thus bidirectional. Afferent and efferent fibres are intertwined to form the renal nerve that runs along the renal artery, partly attached to its adventitia. Sympathetic outflow regulates renal vascular resistance, renin release, and sodium re-absorption [2], [3], [4].

During the past decade, renal nerve radio-ablation through the renal artery has gained much attention as a potential therapy for the treatment of systemic hypertension resistant to pharmacological treatments. Reducing the sympathetic drive to kidneys is expected to lower peripheral vascular resistance while enhancing natriuresis. On the other hand, blocking the afferent signaling of the renal nerve would inhibit the renin-angiotensin-aldosterone system activation. After initial positive results [5], [6], and a large clinical trial not confirming the efficacy of this approach [7], further studies have shown a clear antihypertensive effect of renal nerve ablation [8], [9], [10], [11] persisting for three years [12], [13]. Historically, reversible and tunable alternatives have been preferred in clinical practice to ablative approaches, such as in the case of deep brain stimulation. As regards renal nerves, they might be feasibly modulated with electrical stimulation to produce desirable clinical outcomes, using for instance an intravascular, minimally invasive approach. Yet, this strategy would require a deeper understanding of the role played by the renal nerve in cardiovascular physiology. The classical approach has been based on electrical stimulation, showing the effects of sympathetic renal nerve activity on renal and intrarenal hemodynamics, tubular solute, water reabsorption and renin release [3]. While those studies have provided invaluable insights into the mechanisms of renal control, they were generally based on invasive experimental approaches not easily translatable to the clinical scenario. Moreover, those observations were focused on renal, rather than cardiovascular responses. A few studies [14], [15], [16], [17], [18], [19], [20] employed intravascular electrodes to stimulate the renal nerve through the renal artery wall, showing an increase in BP. Nevertheless, the description they provided was not extensive, as short periods of stimulation were used, the representation of the temporal dynamics of the systolic and diastolic BP changes as well as heart rate were limited (with one exception) to a single point at the end of the stimulation, and the effects of different stimulation parameters were not examined.

The aim of the present study was to test whether the hemodynamic response to trans-vascular electrical stimulation of the renal nerve displays heterogeneity, variations over time and dependence on stimulation parameters. Toward this goal we measured arterial systolic, diastolic, and pulse pressures and employed a post-processing approach capable of mitigating the oscillations related to the breathing cycle, thus allowing the visualization and characterization of small transient alterations.

II. RESULTS

A total of 7 pigs were used during this study. A stimulation catheter was employed to deliver electrical stimulations either

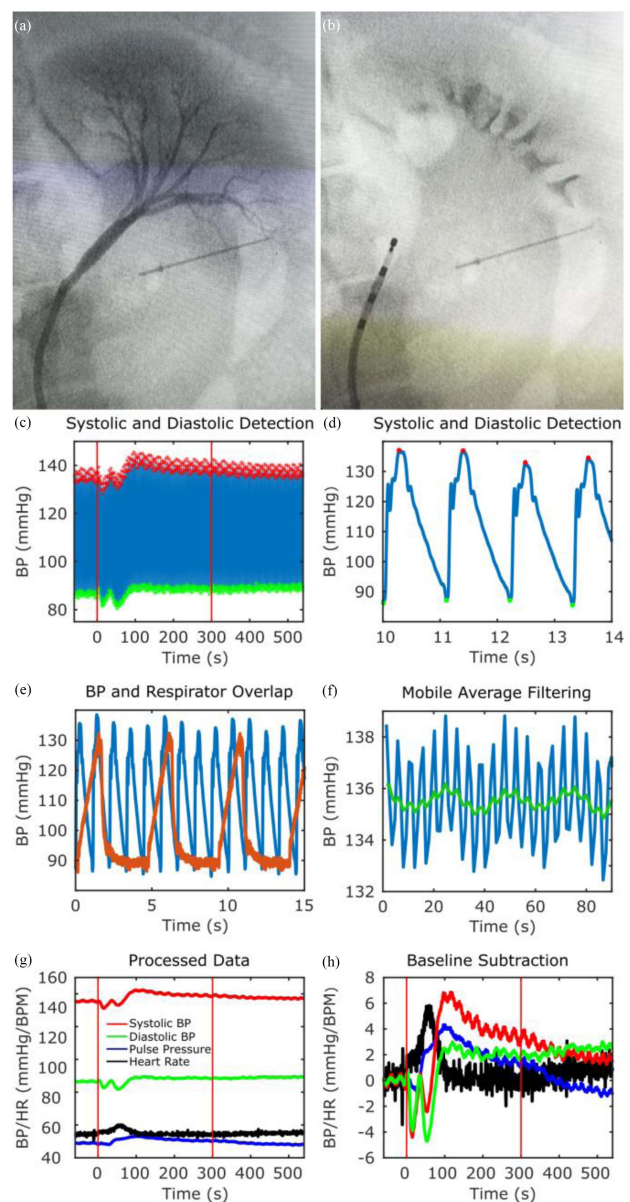


FIGURE 1. Experimental setup and hemodynamics recording and processing. (a) fluoroscopy image of contrast medium perfusing the renal artery. The straight line visible in the lower right side is a needle taped to the surface of the animal abdomen to provide a visual reference. (b) fluoroscopy image of the stimulation catheter advancing in the renal artery. (c) detection of systolic and diastolic blood pressure (BP) values across an entire recording period. Vertical red lines indicate the beginning and the end of the stimulation. (d) systolic and diastolic BP waveforms recorded for a few heartbeats. (e) superimposition of BP and respirator pressure waveforms. (f) reduction of oscillations related to the respiratory cycle obtained with moving average filtering. (g) superimposition of systolic and diastolic BP, pulse pressure and heart rate (HR). (h) superimposition of systolic and diastolic BP, pulse pressure and HR after baseline normalization.

at different locations along the renal artery while maintaining constant parameters, or in a fixed location with different combinations of intensity, frequency and pulse width (PW). Systolic, diastolic pressure and pulse pressure (PP) were measured over the entire duration of the experiment.

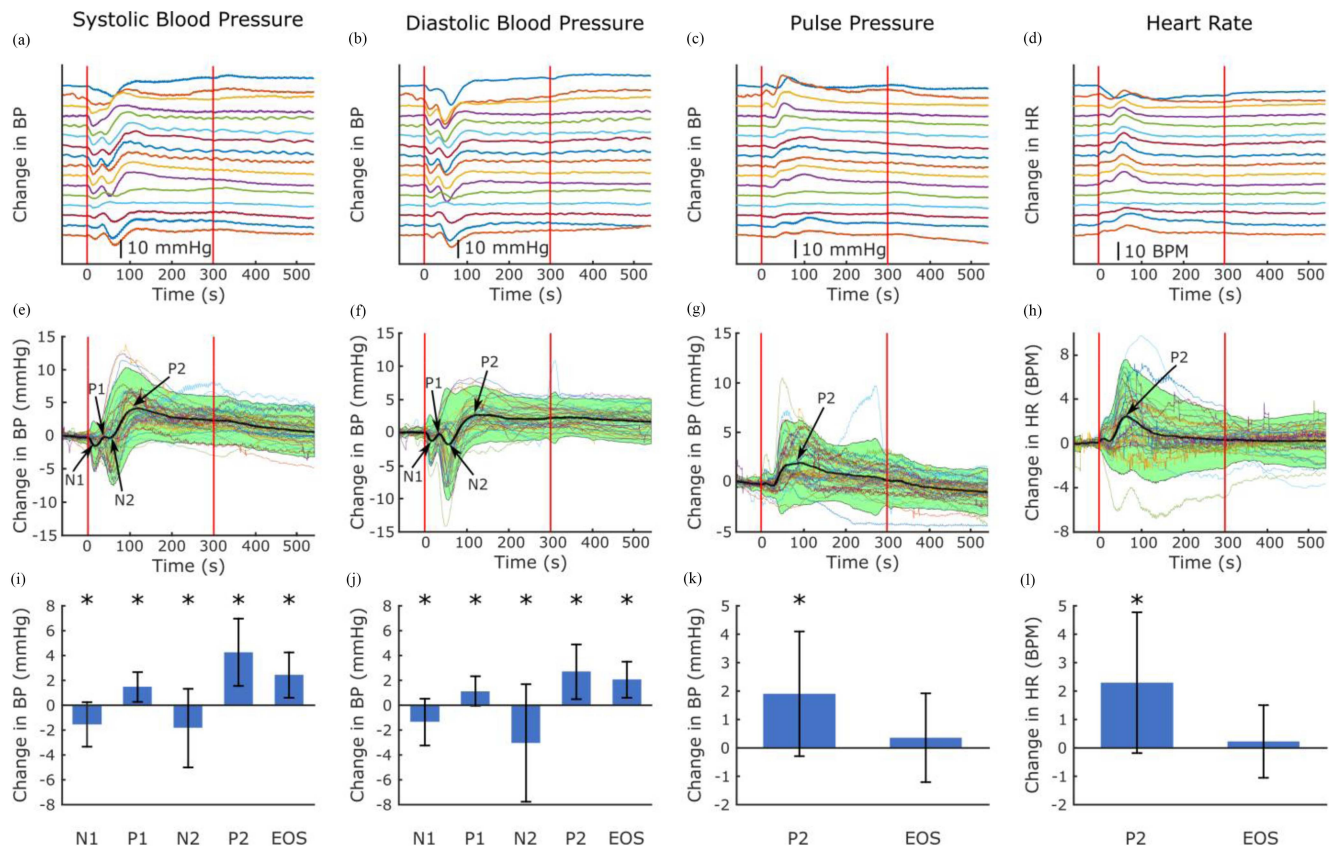


FIGURE 2. Hemodynamic response variability. (a), (b), (c), and (d) changes in systolic and diastolic blood pressure (BP), pulse pressure (PP) and heart rate (HR) elicited by electrical stimulations delivered at different points along the renal artery. Each curve corresponds to a specific point, from the most proximal (top curve) to the most distal (bottom). The electrode was advanced from point to point by 2 mm steps. Red vertical lines indicate the beginning and the end of the stimulation. (e), (f), (g), and (h) superimposition of 43 responses obtained in 4 animals. Stimulations were delivered at 30 mA, 20 Hz and 5 ms pulse width. The black curve represents the average change. The shaded area \pm two SD. (i), (j), (k), and (l) average \pm standard error of the response magnitude for the different peaks. Asterisks indicate statistical difference from zero. P values are reported in Table 1 ($n = 43$ from 4 animals). End of Stimulation (EOS) represents the mean value during the last 30 seconds of stimulation.

The pattern of BP changes during electrical stimulation was complex, being characterized by negative and positive peaks preceding a phase of more stable augmentation (Fig. 1(g) and (h)). These features were not always present (i.e., some stimulations did not produce some or any of the initial peaks), whereas the “long term” response was sustained during stimulation in some cases, while in others a partial reduction was observed even before stopping the stimulation.

In 4 animals we stimulated the nerve using fixed parameters (30 mA, 20 Hz, 5 ms PW) while moving the catheter along the renal artery by 2 mm steps. As shown in Fig. 2(a), (b), (c), and (d), some degree of variability was observed among the hemodynamic responses to stimulations applied at different sites of the artery.

We sought to define the average pattern of the hemodynamic response and of its variability by superimposing the traces obtained from the stimulations delivered while moving the catheter ($n = 43$ from 4 animals) and averaged them over time (thick black line in Fig. 2(e), (f), (g), and (h)). As shown in Fig. 2(e) and (f), systolic and diastolic BP responses to stimulation displayed an initial negative peak (N1) followed

by a positive deflection (P1) and a second negative peak (N2). After these initial transient responses, BP values reached a maximum level (P2) followed by a partial reduction that was sustained until the stimulation was stopped. In contrast, the response pattern of PP and HR appeared simpler, with a single positive peak (named P2 for convenience, since it appears after the initial systolic and diastolic peaks). The time elapsed between the beginning of the stimulation and each peak is reported in Table 1.

To characterize numerically these responses, we measured the changes in systolic and diastolic BP, PP and HR measured at the above-mentioned time points ($n = 43$ from 4 animals). To better characterize the initial transient variations, P1 amplitude was calculated as the difference between the BP value at P1 and at N1, and N2 amplitude as the difference between the BP value at N2 and at P1. To evaluate the stability of the response during stimulation we also measured the amplitude of the “long term” phase by averaging the last 30 seconds before the end of the stimulation (EOS). As shown in Fig. 2(i), (j), (k), and (l), changes from baseline were statistically significant for all the measured time points and variables, apart

TABLE 1. Time Elapsed From the Beginning of Stimulation and Significance for Each of the Identified Peaks (n = 43 From 4 Animals)

| Peak | N1 | P1 | N2 | P2 | EOS |
|-----------------|----------|----------|----------|----------|----------|
| Systolic BP | | | | | |
| Delay (s) | 18.9 | 40.1 | 51.1 | 118.6 | NA |
| p-Val | 1.22E-06 | 4.46E-10 | 5.90E-04 | 5.15E-13 | 8.20E-11 |
| Diastolic BP | | | | | |
| Delay (s) | 16 | 35.1 | 56.5 | 124.1 | NA |
| p-Val | 4.19E-05 | 1.44E-07 | 1.45E-04 | 6.01E-10 | 1.34E-11 |
| Differential BP | | | | | |
| Delay (s) | NA | NA | NA | 96.2 | NA |
| p-Val | | | | 1.11E-06 | 0.131 |
| HR | | | | | |
| Delay (s) | NA | NA | NA | 64.1 | NA |
| p-Val | | | | 3.38E-07 | 0.244 |

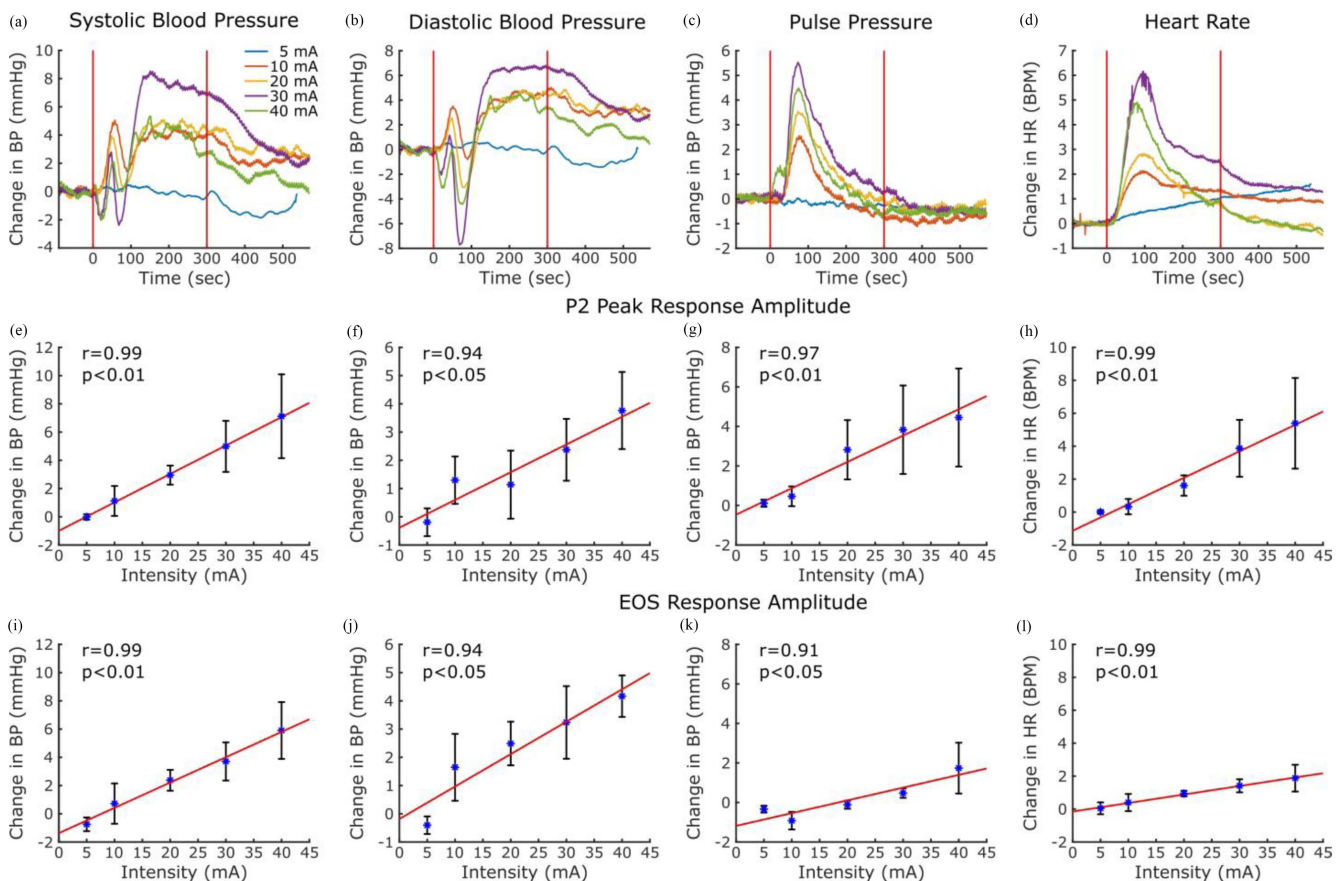


FIGURE 3. Hemodynamic responses to varying stimulations intensities. (a), (b), (c), (d) examples of blood pressure (BP) and heart rate (HR) responses to stimulations of different intensity in one animal. Red vertical lines indicate the beginning and the end of the stimulation. (e), (f), (g), (h) average \pm standard error of the magnitude of P2 evoked by different stimulation intensities. (i), (j), (k), (l) average \pm standard error of the magnitude of the response at the end of stimulation (EOS) at different intensities. Pearson coefficient and relative significance level are reported for each correlation. (n = 4 from 4 animals).

from EOS for PP and HR. Significance values are reported in Table 1.

We then evaluated the dependency of P2 and EOS on stimulation intensity, frequency, and pulse width. In 4 animals we applied stimulations with varying intensity, while keeping

frequency and PW constant. Fig. 3 shows a relatively linear relationship between stimulation intensity and hemodynamic responses, both for P2 (Fig. 4(e), (f), (g), (h)) and EOS (Fig. 4(i), (j), (k), and (l)). We observed an almost complete absence of responses at the lowest amplitude.

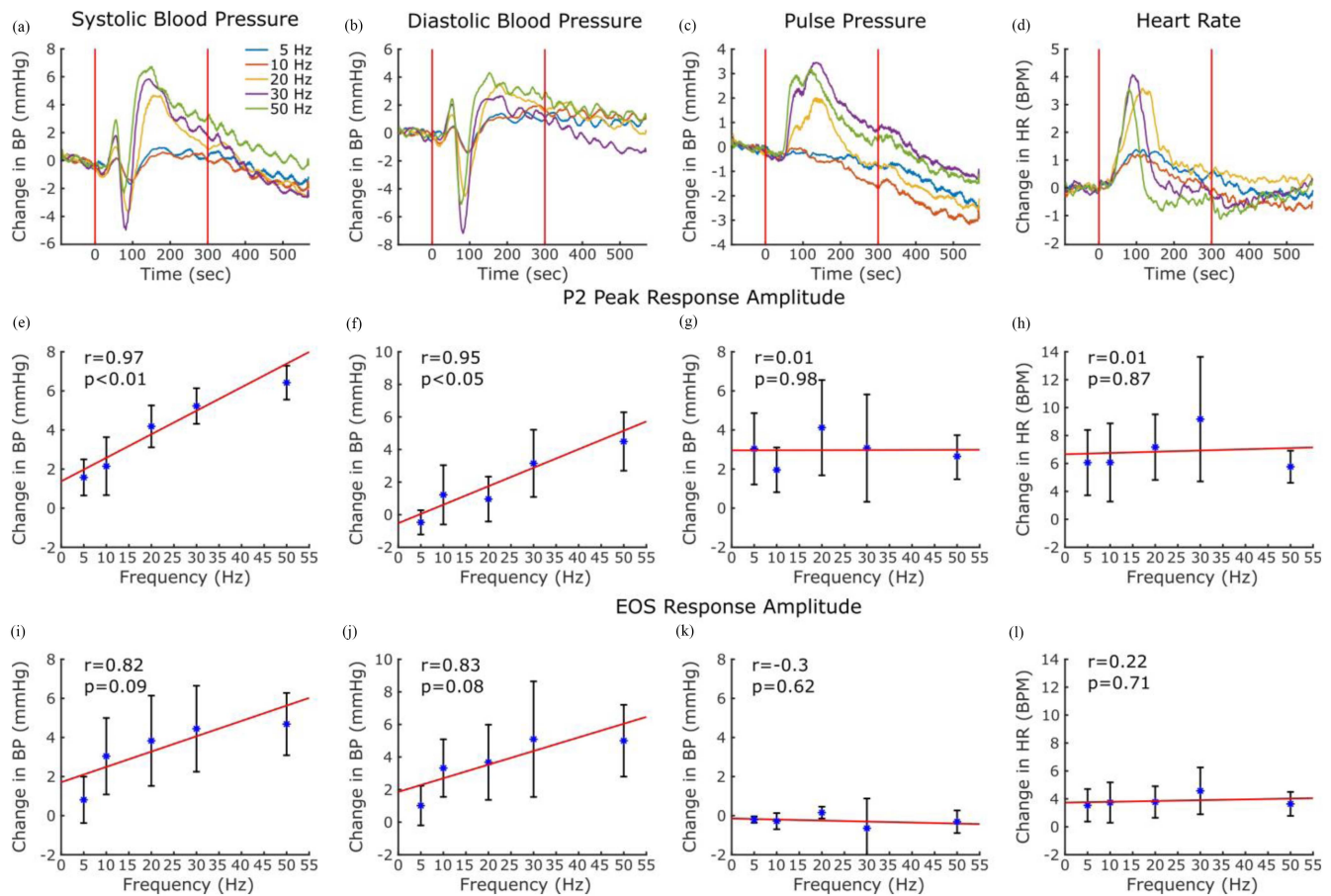


FIGURE 4. Hemodynamic responses to varying stimulation frequencies. (a), (b), (c), (d) example of blood pressure (BP) and heart rate (HR) responses to stimulations at different frequencies in one animal. Red vertical lines indicate the beginning and the end of the stimulation. (e), (f), (g), (h) average \pm standard error of the magnitude of P2 evoked by different stimulation frequencies. (i), (j), (k), (l) average \pm standard error of the magnitude of the response at the end of stimulation (EOS) at different frequencies. Pearson coefficient and relative significance level are reported for each correlation. (n = 4 from 4 animals).

In 4 animals we applied stimulations with varying frequency, while keeping intensity and PW constant. In contrast to low intensities, hemodynamic changes were elicited even at lower stimulation frequencies, as shown in Fig. 4. Interestingly, whereas systolic and diastolic BP appears to increase linearly with the stimulation frequency (Fig. 5(e) and (f)), a similar relationship did not occur for PP and HR (Fig. 4(g) and (h)).

In 3 animals we varied the PW, while keeping intensity and frequency constant. Fig. 5 shows that small or no responses were observed at PW of 1 ms with a relatively linear increase of the evoked response to increasing levels of PW.

We compared heart rate variability (HRV), an established index of sympathetic/parasympathetic tone [21], measured during and after stimulation using n = 43 recording from 4 animals. As shown in Table 2, the standard deviation of the intervals between heartbeats (SDNN) and HRV index (HRVI) were significantly elevated during stimulation when compared to the post-stimulation period. No significant differences were observed relative to the low to high frequencies ratio or to the high frequencies calculated around the breathing frequency.

TABLE 2. Mean \pm Standard Deviation of the Heart Rate Variability Outcomes

| | ON | POST | p-Val |
|-------|-------------------|------------------|----------|
| SDNN | 21.88 \pm 10.58 | 14.19 \pm 6.81 | 2.48E-05 |
| HRVI | 4.41 \pm 1.56 | 3.5 \pm 0.99 | 2.23E-05 |
| LF/HF | 0.35 \pm 0.14 | 0.34 \pm 0.13 | 0.92 |
| HF B | 0.33 \pm 0.04 | 0.31 \pm 0.04 | 0.11 |

III. DISCUSSION

The results of this study show a complex hemodynamic response to trans-vascular electrical stimulation of the renal nerve. Changes in BP were characterized by different phases, with negative and positive peaks. For example, the hemodynamic responses changed within the same animal when stimulation was applied at different sites along the renal artery.

A. EFFECT OF STIMULATION PARAMETERS

To characterize the hemodynamic response to trans-vascular electrical stimulation of the renal nerve, we tested the influence of stimulation parameters by altering one parameter at

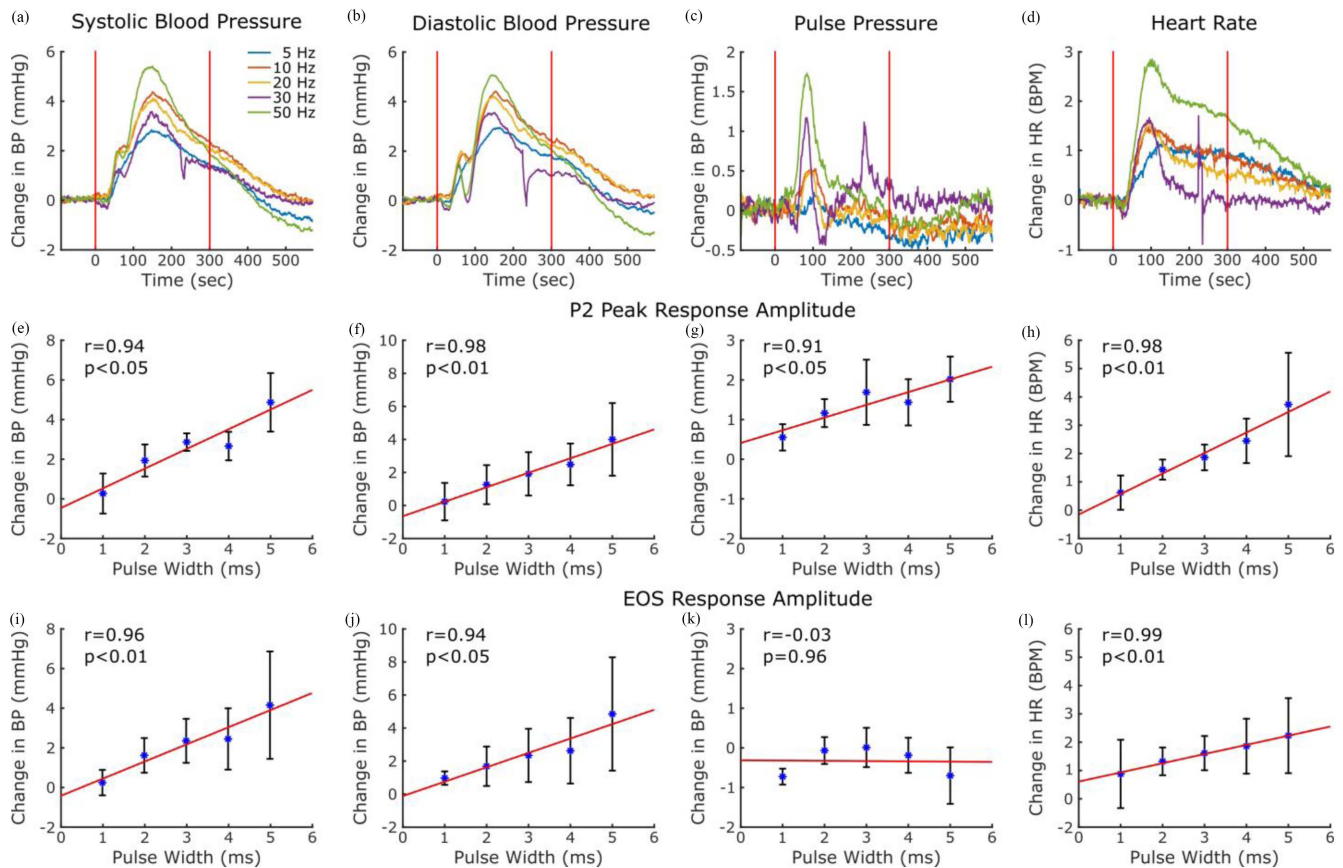


FIGURE 5. Hemodynamic responses to varying stimulation pulse widths. (a), (b), (c), (d) example of blood pressure (BP) and heart rate (HR) responses to stimulations at different pulse widths in one animal. Red vertical lines indicate the beginning and the end of the stimulation. (e), (f), (g), (h) average \pm standard error of the magnitude of P2 evoked by different stimulation pulse widths. (i), (j), (k), (l) average \pm standard error of the magnitude of the response at the End of Stimulation (EOS) at different pulse widths. Pearson coefficient and relative significance level are reported for each correlation. ($n = 3$ from 3 animals).

the time. We observed a progressive increase of the hemodynamic response mirroring the increase in stimulation amplitude, frequency, and PW. The almost complete absence of response at the lowest intensity value (5 mA) suggests that the electrical field generated by the stimulator needs to extend relatively far from the electrode to activate renal nerve fibres. This is in accordance with the available histologic data documenting that only a very small fraction of the fibres is located within the first half a millimeter of tissue surrounding the renal artery, both in swine [22] and in humans [23], [24]. The sympathetic fibres of the renal nerve are not organized in a single bundle, like in a somatic nerve, but are rather distributed within a relatively wide radius and some have been found as far as 1 cm distant from the outer surface of the vessel wall [22]. Interestingly, the increase in hemodynamic responses seems to correlate almost linearly with the increase in the delivered current. This suggests that progressive recruitment of additional fibres occurs as the stimulation amplitude is increased. Moreover, the response amplitude did not reach a plateau, which suggests that additional the fibres, likely those furthest from the vessel wall, could not be recruited even at the highest current intensity.

The current intensity tested during our study was higher than expected and larger than those reported in canine models [14], [15], [16], [17], [19], albeit comparable. While the distance between the nerve fibers and the renal artery is not very large, it seems that the obstacle represented by the interposed arterial wall, as well as possible shunting effects due to blood flow, can be overcome only by conspicuous current intensities. Moreover, we utilized bipolar stimulation with the smallest inter-electrode distance (5 mm), which, different from monopolar stimulation, is characterized by a much more limited spread of the current generated by the electrodes. It is possible that trans-vascular stimulation modalities that produce substantially wider activation fields would prove more efficient.

When specifically testing the impact of stimulation frequencies, we found hemodynamic responses even at the lower values (i.e., 5 and 10 Hz). Interestingly, whereas systolic and diastolic BP increased in a seemingly linear fashion in response to progressively higher stimulation frequencies, PP and HR responded differently. This is surprising, since, if the changes in PP and HR were entirely secondary to the systolic and diastolic BP alterations, one could expect them to follow

the same pattern. Whereas such discrepancy could hint at the involvement of separate mechanisms, the limited number of data points prevents further interpretations.

Finally, we tested the specific impact of PW on the hemodynamic responses. In this case, all the measured hemodynamic parameters increased linearly in response to progressively longer PW. Since smaller axons have larger chronaxie values, increases in PW may recruit progressively larger numbers of fibres characterized by progressively smaller axonal diameters. The need for such long PW values strongly suggests that most of the observed effects are likely mediated by small diameter unmyelinated fibres known to have a chronaxie of about 2 ms [25]. Indeed, this is consistent with the fact that the sympathetic nervous system post-ganglionic neurons are C-fibres [26].

B. HEART RATE VARIABILITY

The difference in HRV between the stimulation and the post-stimulation period is not surprising, considering that HR undergoes a transient increase, as shown in Fig. 2(a). Such an alteration will inherently increase the standard deviation of the inter-beat intervals (IBI) as well as widen the IBI distribution as indicated by the increase in SDNN and HRVI. Likewise, the absence of significant changes in the LF/HF ratio or in the HF power at the breathing frequency is not surprising. As the stimulation-induced HR alterations occur over a relatively long time, their contribution to the power spectrum is well below the range of the frequencies used in the frequency domain analysis of the IBI variability.

C. GENERAL CONSIDERATIONS

A comparison with the existing literature is not straightforward, due to the variability in the stimulation parameters and duration utilized by other authors. In general, shorter stimulations, i.e., one [14], [15], [17], [19], [20] or two minutes [16] long, were used and often only single BP values recorded at the end of the stimulation. The previously reported increases in BP are larger than those observed in the current study and, interestingly, they were detectable 1 minute after the beginning of the stimulation, a time when, in our study, we rather observed the occurrence of N2. More in accordance with our results, others reported responses starting either “a few seconds” [15] or 15–30 seconds [14] after the beginning of the stimulation. When a description of the time course was provided [20], the responses appeared monotonic. It is hard to reconcile these discrepancies and they are likely related to differences in models (porcine versus canine), stimulation parameters, or anesthesia. We used the gas anesthetic sevoflurane, while others used sodium thiopental [14], [19], sodium pentobarbital [17], [20], or isoflurane [15], [16]. Additionally, in our study the initial peaks often became evident only after attenuating ventilation-related BP oscillations. Our results seem to confirm in pigs that BP is elevated during long term renal nerve trans-vascular stimulation, while we characterized more in depth the time course of hemodynamic changes.

Our data can provide at least two indications for the development of an intravascular renal nerve stimulation strategy. Firstly, there is a clear need for purpose-built stimulation electrodes that closely adhere to the entire intravascular wall surface, thus minimizing the distance from nerve fibres and covering an adequate distance along the vessel. Secondly, the ideal stimulation pattern would depend on the desired cardiac effect. For instance, if the goal is a long-term increase in systolic and diastolic BP, this may be achieved by employing high values for all 3 stimulation parameters (Intensity, frequency, and PW). If, on the other hand, the goal is a short-term transient increase in PP and HR, strong pulses with a long pulse duration at a low frequency would be more indicated. Further research is needed to obtain an increase in the magnitude of cardiac response while reducing the stimulation intensities.

D. LIMITATIONS

Several study limitations should be acknowledged. The presence of stimulation artifacts in the ECG recordings required us to estimate the IBI from the pressure signal. This approach is inherently less precise and, while it presents no problems when calculating HR, additional caution must be taken for HRV assessment, as it could increase the inherent variability of the measurement. As bladder pressure was not monitored during stimulation, we cannot rule out that part of the observed effect could be due to an induced increase in bladder pressure influencing cardiac activity via afferent fibers. Furthermore, it is likely that the amplitude of the observed responses and the pattern of some of the time-dependent changes were blunted by gas anesthesia. Other types of anesthesia utilized in the past for this type of animal studies are no longer an option. Another limitation relates to the clinical standard electrode catheter employed by us, which was not specifically designed for a transvascular nerve stimulation, and might in part explain the need for high current intensities specifically. Finally, we did not compare hemodynamic changes measured in the absence and the presence of a pharmacological blockade of cardiac and vascular adrenergic response. Although desirable, these tests would have rendered difficult restoring baseline hemodynamic values before each new stimulation modality could be tested.

IV. CONCLUSION

Our results provide important insights in the complexity of hemodynamic response to electrical renal nerve stimulation that did not emerge in previous studies and might contribute to the design of conservative and tunable therapeutic strategies as an alternative to renal nerve ablation.

V. METHODS

A. SURGICAL PROCEDURE

The animal protocol was approved by institutional ethical committee (N. 1117) and by the Italian Ministry of Health, and was in accordance with the Italian law (D.lgs. 26/2014).

We used 7 healthy male farm pig (*Sus Scrofa*) with a body weight ranging between 30 and 35 kg. They were pre-medicated with a cocktail of zolazepam (5 mg/kg) and tiletamine (5 mg/kg), anesthetized with propofol (2 mg/kg intravenously), intubated and artificially ventilated at the rate of 13 breath/minute. Anesthesia was maintained with 1-2% sevoflurane vaporized in the respiratory 50% air-50% oxygen mixture. The animals were infused with 0.9 % NaCl solution over the duration of the experiment to prevent dehydration. A saline-filled catheter was inserted in the carotid artery to measure central arterial blood pressure, data were sampled at 1.5 kHz and saved for analysis. A 6Fr amplatz right (AR1.0) guide catheter (Medtronic, USA) was inserted in the femoral artery, advanced and positioned in the right renal artery under X-ray fluoroscopic guidance. Contrast medium was injected to confirm the correct positioning of the catheter (Fig. 1(a)). Subsequently, a 4-cylindrical contacts stimulation catheter (Supreme, Abbott Chicago, IL, USA) was introduced in the renal artery to deliver electrical stimulations (Fig. 1(b)). This catheter has a 1.33 mm diameter and 4 electrodes, one covering the tip and 3 rings 2 mm long, spaced 5 mm apart.

The stimulation catheter was connected to a constant current linear stimulator (Stmisola, Biopac, Goleta, CA, USA), set with output mode “I”, $z=100 \Omega$. The stimulator was controlled using a digital to analog converter (National Instruments, Austin, Texas, USA). The DAQ was controlled using Matlab (Mathworks, Natick, MS, USA) at a sampling rate of 5000 Hz.

At the end of the study, animals were anesthetized with a bolus of propofol 1% (5 mg/Kg) and euthanized by injection of 10% KCl (20 ml) to stop the heart in diastole.

B. STIMULATION PROTOCOL

Stimulation was delivered using the most distal contact as the cathode and the immediately adjacent contact as the anode. The electrical stimuli consisted of cathodic first, biphasic symmetric rectangular waveforms with an intensity varying from 5 to 40 mA, a frequency between 5 and 50 Hz and a PW between 1 and 5 ms. In one set of experiments, stimulations were delivered at different points within the renal artery by moving the tip of the catheter from the proximal (near the aorta) to the distal end (toward the kidney) with 2 mm steps. During these experiments, the stimulation was delivered at 30 mA, 20 Hz and a PW of 5 ms. In a second set of experiments, the position of the catheter was fixed leaving it in the proximal segment of the artery, while varying intensity (5, 10, 20, 30, 40 mA, 20 Hz, 5 ms PW), frequency (5, 10, 20, 30, 50 Hz, 30 mA, 5 ms PW) or PW (1, 2, 3, 4, 5 ms, 30 mA, 20 Hz) of the stimuli.

C. BLOOD PRESSURE ANALYSIS

During all the experiments, baseline hemodynamic values were recorded for 90 seconds at baseline, than stimulation was started and held for 5 minutes, followed by at least 5 minutes of pause to allow the return of BP to baseline levels (Fig. 1(c)). Systole and diastole were detected for each

heartbeat (Fig. 1(d)). As expected, mechanical ventilation caused BP fluctuations synchronous with lung inflation and deflation (Fig. 1(e)). To reduce this confounding effect, systolic and diastolic BP were filtered using a moving average filter with a window size corresponding to the number of heart beats recorded during each cycle of the respirator at baseline (Fig. 1(f)). To ensure consistency in the timing of each heartbeat detection, the BP signal was low passed with a 4th order Butterworth filter and a cut-off frequency of 5 Hz. Systolic peaks in this smoothed BP trace were identified and instantaneous HR was derived based on the inverse of the peak-to-peak time interval. As the respiratory cycle also affected HR, the moving average filter used for systolic and diastolic BP was applied to the HR to minimize the impact of its oscillations. To allow a better comparison between different stimulations, systolic and diastolic BP and HR traces were normalized subtracting the average values calculated over the baseline phase (Fig. 1(g) and (h)). PP was also calculated as the difference between systolic and diastolic BP.

D. HEART RATE VARIABILITY ANALYSIS

To provide a more comprehensive picture, we analyzed HRV, albeit this analysis was affected by important limitations. Stimulation artifacts interfered significantly with ECG recordings and could not be used to identify R-R intervals. The beginning of the sharp rise in BP associated with each heartbeat was instead used as proxy to calculate inter-beat intervals (IBIs). IBIs were used to calculate the standard deviation of the IBI (SDNN), the heart rate variability index (HRVI) and the ratio between the power in the low (0.04–0.15 Hz) and the high frequencies (0.15–0.40 Hz) in the IBI spectrum (LF/HF) [21]. Additionally, we calculated the high frequencies in a 0.1 Hz interval centered around the breathing frequency of 0.22 Hz (0.17–0.27 Hz), normalized by the total power (0.04–0.4 Hz). As the baseline period used for the acquisitions was shorter than the 5 minutes suggested for HRV calculations, the stimulation period was compared only to the post-stimulation period. HRV was calculated based on the data obtained while moving the electrode position, as this data subset better represent the variability of the responses to trans-vascular renal nerve stimulation.

E. STATISTICAL ANALYSIS

Data are reported as mean \pm standard deviation. The average of peak changes in BP and HR was normalized to baseline values and relative changes vs 0 (null hypothesis) were tested using the one sample t test. To evaluate the dependency of the hemodynamic responses on stimulation parameters, we calculated the corresponding Pearson’s coefficients and the associated significance values. Changes in HRV measurements between the stimulation period and the post stimulation period were tested using paired two sample t test.

REFERENCES

- [1] C. Bernard, *Leçons Sur Les Propriétés Physiologiques et Les Altérations Pathologiques Des Liquides de L'organisme*. Paris, France: Baillière, 1859, doi: [10.5962/bhl.title.1814](https://doi.org/10.5962/bhl.title.1814).
- [2] E. J. Johns, U. C. Kopp, and G. F. DiBona, "Neural control of renal function," *Comprehensive Physiol.*, vol. 1, no. 2, pp. 731–767, Apr. 2011, doi: [10.1002/cphy.c100043](https://doi.org/10.1002/cphy.c100043).
- [3] J. W. Osborn and J. D. Foss, "Renal nerves and long-term control of arterial pressure," *Comprehensive Physiol.*, vol. 7, no. 2, pp. 263–320, Mar. 2017, doi: [10.1002/cphy.c150047](https://doi.org/10.1002/cphy.c150047).
- [4] J. W. Osborn, R. Tyshynsky, and L. Vulchanova, "Function of renal nerves in kidney physiology and pathophysiology," *Annu. Rev. Physiol.*, vol. 83, pp. 429–450, Feb. 2021, doi: [10.1146/annurev-physiol-031620-091656](https://doi.org/10.1146/annurev-physiol-031620-091656).
- [5] H. Krum et al., "Catheter-based renal sympathetic denervation for resistant hypertension: A multicentre safety and proof-of-principle cohort study," *Lancet*, vol. 373, no. 9671, pp. 1275–1281, Apr. 2009, doi: [10.1016/S0140-6736\(09\)60566-3](https://doi.org/10.1016/S0140-6736(09)60566-3).
- [6] Symplicity HTN-2 Investigators et al., "Renal sympathetic denervation in patients with treatment-resistant hypertension (The Symplicity HTN-2 Trial): A randomised controlled trial," *Lancet*, vol. 376, no. 9756, pp. 1903–1909, Dec. 2010, doi: [10.1016/S0140-6736\(10\)62039-9](https://doi.org/10.1016/S0140-6736(10)62039-9).
- [7] D. L. Bhatt et al., "A controlled trial of renal denervation for resistant hypertension," *New England J. Med.*, vol. 370, no. 15, pp. 1393–1401, Apr. 2014, doi: [10.1056/NEJMoa1402670](https://doi.org/10.1056/NEJMoa1402670).
- [8] M. Böhm et al., "Efficacy of catheter-based renal denervation in the absence of antihypertensive medications (SPYRAL HTN-OFF MED Pivotal): A multicentre, randomised, sham-controlled trial," *Lancet*, vol. 395, no. 10234, pp. 1444–1451, May 2020, doi: [10.1016/S0140-6736\(20\)30554-7](https://doi.org/10.1016/S0140-6736(20)30554-7).
- [9] D. E. Kandzari et al., "Effect of renal denervation on blood pressure in the presence of antihypertensive drugs: 6-month efficacy and safety results from the SPYRAL HTN-ON MED proof-of-concept randomised trial," *Lancet*, vol. 391, no. 10137, pp. 2346–2355, Jun. 2018, doi: [10.1016/S0140-6736\(18\)30951-6](https://doi.org/10.1016/S0140-6736(18)30951-6).
- [10] M. Azizi et al., "Endovascular ultrasound renal denervation to treat hypertension (RADIANCE-HTN SOLO): A multicentre, international, single-blind, randomised, sham-controlled trial," *Lancet*, vol. 391, no. 10137, pp. 2335–2345, Jun. 2018, doi: [10.1016/S0140-6736\(18\)31082-1](https://doi.org/10.1016/S0140-6736(18)31082-1).
- [11] M. Azizi et al., "Ultrasound renal denervation for hypertension resistant to a triple medication pill (RADIANCE-HTN TRIO): A randomised, multicentre, single-blind, sham-controlled trial," *Lancet*, vol. 397, no. 10293, pp. 2476–2486, Jun. 2021, doi: [10.1016/S0140-6736\(21\)00788-1](https://doi.org/10.1016/S0140-6736(21)00788-1).
- [12] D. L. Bhatt et al., "Long-term outcomes after catheter-based renal artery denervation for resistant hypertension: Final follow-up of the randomised SYMPPLICITY HTN-3 Trial," *Lancet*, vol. 400, no. 10361, pp. 1405–1416, Oct. 2022, doi: [10.1016/S0140-6736\(22\)01787-1](https://doi.org/10.1016/S0140-6736(22)01787-1).
- [13] F. Mahfoud et al., "Long-term efficacy and safety of renal denervation in the presence of antihypertensive drugs (SPYRAL HTN-ON MED): A randomised, sham-controlled trial," *Lancet*, vol. 399, no. 10333, pp. 1401–1410, Apr. 2022, doi: [10.1016/S0140-6736\(22\)00455-X](https://doi.org/10.1016/S0140-6736(22)00455-X).
- [14] M. Chinushi et al., "Blood pressure and autonomic responses to electrical stimulation of the renal arterial nerves before and after ablation of the renal artery," *Hypertension*, vol. 61, no. 2, pp. 450–456, Feb. 2013, doi: [10.1161/HYPERTENSIONAHA.111.00095](https://doi.org/10.1161/HYPERTENSIONAHA.111.00095).
- [15] M. Madhavan et al., "Transvenous stimulation of the renal sympathetic nerves increases systemic blood pressure: A potential new treatment option for neurocardiogenic syncope," *J. Cardiovasc. Electrophysiol.*, vol. 25, no. 10, pp. 1115–1118, Oct. 2014, doi: [10.1111/jce.12466](https://doi.org/10.1111/jce.12466).
- [16] N. Naksuk et al., "Blood pressure responses to endovascular stimulation: A potential therapy for autonomic disorders with vasodilatation," *J. Cardiovasc. Electrophysiol.*, vol. 27, no. 9, pp. 1078–1085, Sep. 2016, doi: [10.1111/jce.13018](https://doi.org/10.1111/jce.13018).
- [17] J. Lu et al., "Selective proximal renal denervation guided by autonomic responses evoked via high-frequency stimulation in a preclinical canine model," *Circulation Cardiovasc. Interv.*, vol. 8, no. 6, Jun. 2015, Art. no. e001847, doi: [10.1161/CIRCINTERVENTIONS.115.001847](https://doi.org/10.1161/CIRCINTERVENTIONS.115.001847).
- [18] P. Gal, M. R. de Jong, J. J. J. Smit, A. Adiyaman, J. A. Staessen, and A. Elvan, "Blood pressure response to renal nerve stimulation in patients undergoing renal denervation: A feasibility study," *J. Hum. Hypertension*, vol. 29, no. 5, pp. 292–295, May 2015, doi: [10.1038/jhh.2014.91](https://doi.org/10.1038/jhh.2014.91).
- [19] M. Chinushi, O. Saitoh, A. Sugai, A. Oikawa, J. Watanabe, and H. Furushima, "Enhanced arrhythmogenic potential induced by renal autonomic nerve stimulation: Role of renal artery catheter ablation," *Heart Rhythm*, vol. 17, no. 1, pp. 133–141, Jan. 2020, doi: [10.1016/j.hrthm.2019.07.029](https://doi.org/10.1016/j.hrthm.2019.07.029).
- [20] H. Liu et al., "Selective renal denervation guided by renal nerve stimulation in canine," *Hypertension*, vol. 74, no. 3, pp. 536–545, Sep. 2019, doi: [10.1161/HYPERTENSIONAHA.119.12680](https://doi.org/10.1161/HYPERTENSIONAHA.119.12680).
- [21] "Heart rate variability. Standards of measurement, physiological interpretation, and clinical use. Task force of the European society of cardiology and the north american society of pacing and electrophysiology," *Eur. Heart J.*, vol. 17, no. 3, pp. 354–381, Mar. 1996.
- [22] A. Tellez et al., "Renal artery nerve distribution and density in the porcine model: Biologic implications for the development of radiofrequency ablation therapies," *Transl. Res.: J. Lab. Clin. Med.*, vol. 162, no. 6, pp. 381–389, Dec. 2013, doi: [10.1016/j.trsl.2013.07.002](https://doi.org/10.1016/j.trsl.2013.07.002).
- [23] A. Ds, D. Nl, and M. Fo, "Micro-anatomy of the renal sympathetic nervous system: A human postmortem histologic study," *Clin. Anatomy*, vol. 25, no. 5, pp. 628–633, Jul. 2012, doi: [10.1002/ca.21280](https://doi.org/10.1002/ca.21280).
- [24] K. Sakakura et al., "Anatomic assessment of sympathetic peri-arterial renal nerves in man," *J. Amer. College Cardiol.*, vol. 64, no. 7, pp. 635–643, Aug. 2014, doi: [10.1016/j.jacc.2014.03.059](https://doi.org/10.1016/j.jacc.2014.03.059).
- [25] D. C. West and J. H. Wolstencroft, "Strength-duration characteristics of myelinated and non-myelinated bulbospinal axons in the cat spinal cord," *J. Physiol.*, vol. 337, pp. 37–50, Apr. 1983, doi: [10.1113/jphysiol.1983.sp014610](https://doi.org/10.1113/jphysiol.1983.sp014610).
- [26] G. Pocock and C. D. Richards, *Human Physiology: The Basis of Medicine*, 2nd ed. Oxford, U.K.: Oxford Univ. Press, 2004.

Open Access funding provided by 'Scuola Superiore "S. Anna" di Studi Universitari e di Perfezionamento' within the CRUI CARE Agreement